Observed decrease in atmospheric mercury explained by global decline in anthropogenic emissions

Yanxu Zhang[a,1], Daniel J. Jacob[a,b], Hannah M. Horowitz[a], Long Chen[a,c], Helen M. Amos[a], David P. Krabbenhoft[d], Franz Slemr[e], Vincent L. St. Louis[f], and Elsie M. Sunderland[a,g]

[a]John A. Paulson School of Engineering and Applied Sciences, Harvard University, Cambridge, MA 02138; [b]Department of Earth and Planetary Sciences, Harvard University, Cambridge, MA 02138; [c]College of Urban and Environmental Sciences, Peking University, Beijing 100871, China; [d]US Geological Survey, Wisconsin Water Science Center, Middleton, WI 53562; [e]Department of Atmospheric Chemistry, Max Planck Institute for Chemistry, Mainz 55128, Germany; [f]Department of Biological Sciences, University of Alberta, Edmonton, AB, Canada T6G 2R3; and [g]Department of Environmental Health, T. H. Chan School of Public Health, Harvard University, Boston, MA 02115

Observations of elemental mercury (Hg^0) at sites in North America and Europe show large decreases (∼1–2% y^{-1}) from 1990 to present. Observations in background northern hemisphere air, including Mauna Loa Observatory (Hawaii) and CARIBIC (Civil Aircraft for the Regular Investigation of the atmosphere Based on an Instrument Container) aircraft flights, show weaker decreases (<1% y^{-1}). These decreases are inconsistent with current global emission inventories indicating flat or increasing emissions over that period. However, the inventories have three major flaws: (*i*) they do not account for the decline in atmospheric release of Hg from commercial products; (*ii*) they are biased in their estimate of artisanal and small-scale gold mining emissions; and (*iii*) they do not properly account for the change in Hg^0/Hg^{II} speciation of emissions from coal-fired utilities after implementation of emission controls targeted at SO_2 and NO_x. We construct an improved global emission inventory for the period 1990 to 2010 accounting for the above factors and find a 20% decrease in total Hg emissions and a 30% decrease in anthropogenic Hg^0 emissions, with much larger decreases in North America and Europe offsetting the effect of increasing emissions in Asia. Implementation of our inventory in a global 3D atmospheric Hg simulation [GEOS-Chem (Goddard Earth Observing System-Chemistry)] coupled to land and ocean reservoirs reproduces the observed large-scale trends in atmospheric Hg^0 concentrations and in Hg^{II} wet deposition. The large trends observed in North America and Europe reflect the phase-out of Hg from commercial products as well as the cobenefit from SO_2 and NO_x emission controls on coal-fired utilities.

mercury | trend | emission | atmosphere

Mercury (Hg) is released to the atmosphere by human activities including coal combustion, mining, and manufacturing and discard of commercial products (1, 2). Hg is transported globally as elemental Hg (Hg^0) in the atmosphere, eventually oxidizing to divalent Hg (Hg^{II}) that deposits to the surface, accumulates in ecosystems, and endangers humans and wildlife when converted to the neurotoxin methylmercury (3, 4). Surface air Hg concentrations in the northern hemisphere declined by 30–40% between 1990 and 2010 (5–7), and similar decreases have been observed in Hg wet deposition fluxes across North America and Western Europe (8, 9). By contrast, global inventories suggest flat or increasing Hg emissions over the last two decades (1, 10). Decreasing reemission of Hg from oceans and soils has been speculated (5, 6). Here we show that the declining atmospheric concentrations can be explained by the phase-out of Hg from commercial products and by shifts in the speciation of Hg emissions driven by air pollution control technologies.

Observed Atmospheric Hg Trends Since 1990

Table 1 compiles observed 1990-to-present trends in atmospheric Hg^0 concentrations and Hg^{II} wet deposition fluxes worldwide, including our own analyses. A general decline in the concentration of Hg^0 is observed at surface sites, continuing to the most recent years. Decreases in atmospheric Hg^0 concentrations range from 1.2 to 2.1% y^{-1} at northern midlatitudes. Trends are weaker and less significant at high northern latitudes above 60° N (−0.9 to +0.1% y^{-1}). Preliminary data from an urban and a remote site in China suggest an increasing trend of about +2% y^{-1} over the last decade (17). Wet deposition trends (available only for North America and Western Europe) are similar to trends in atmospheric concentrations.

Observed Hg^0 concentrations in the free troposphere above 2-km altitude show less significant declines. CARIBIC (Civil Aircraft for the Regular Investigation of the atmosphere Based on an Instrument Container) measurements in the northern hemisphere on commercial aircraft over the past decade (www.caribic-atmospheric.com) indicate a weak decline (−0.6 ± 0.6% y^{-1}) that is not statistically significant ($P > 0.05$). Data from Mauna Loa, Hawaii (3.4 km above sea level), similarly indicate a statistically insignificant decline of −0.9 ± 0.6% y^{-1}. We expect these free tropospheric trends to be representative of the tropospheric background, implying trends observed at surface sites are more influenced by regional sources and thus biased for global trend evaluation.

Significance

Anthropogenic mercury poses risks to humans and ecosystems when converted to methylmercury. A longstanding conundrum has been the apparent disconnect between increasing global emissions trends and measured declines in atmospheric mercury in North America and Europe. This work shows that locally deposited mercury close to coal-fired utilities has declined more rapidly than previously anticipated because of shifts in speciation from air pollution control technology targeted at SO_2 and NO_x. Reduced emissions from utilities over the past two decades and the phase-out of mercury in many commercial products has led to lower global anthropogenic emissions and associated deposition to ecosystems. This implies that prior policy assessments underestimated the regional benefits of declines in mercury emissions from coal-fired utilities.

Table 1. Observed 1990 to present trends in atmospheric Hg⁰ concentrations and HgII wet deposition fluxes since the 1990s

Period	Location (network)	Trend, % y^{-1}[a]	Source
Atmospheric Hg^0 concentrations			
1995 to 2010	Canada (CAMNet)	−1.6 ± 0.8[b,c]	Ref. 7
1996 to 2004	Cape Point, South Africa	−1.3 ± 0.3[c,d]	Ref. 11
1990 to 1996	Wank, Germany	−6.1 ± 1.1[c,d]	Ref. 12
1996 to 2013	Mace Head, Ireland	−1.3 ± 0.2[c,e]	Ref. 13
1990 to 2009	North Atlantic, cruises	−2.5 ± 0.5[c,d]	Ref. 6
	South Atlantic	Not significant	
2000 to 2009	Alert, Canada	−0.9 ± 0.5[f,g]	Ref. 28
	Zeppelin, Norway	Not significant	
2008 to 2013	United States (AMNet)	Not significant[c,e]	This study
2005 to 2013	Experimental Lakes Area, Canada	−2.2 ± 0.6[c,e]	This study
1990 to 2011	Western Europe (EMEP)	−2.1 ± 0.5[c,e]	This study
1994 to 2012	North of 60° N	Not significant[c,e]	This study
2005 to 2014	Free troposphere (CARIBIC)	Not significant[c,e,h]	This study
2002 to 2013	Mauna Loa Observatory, Hawaii	Not significant[c,d]	Ref. 14
Hg^{II} wet deposition			
1996 to 2008	North America (MDN)	Not significant[c,i]	Ref. 9
	Western Europe (EMEP)	−1.5 ± 0.5	
1998 to 2005	Northeast United States (MDN)	−1.7 ± 0.5[c,j]	Ref. 15
	Midwest United States	−3.5 ± 0.7	
	Southeast United States	Not significant	
1996 to 2005	Northeast United States (MDN)	−2.1 ± 0.9[g,k,l]	Ref. 8
	Midwest United States	−1.8 ± 0.3	
	Southeast United States	−1.3 ± 0.3	
	West United States	−1.4 ± 0.4	
2002 to 2008	Northeast United States (MDN)	Not significant[g,l]	Ref. 16
	Midwest United States	Not significant	
2004 to 2010	Northeast United States (MDN)	−4.1 ± 0.5[c,m]	Ref. 26
	Midwest United States	−2.7 ± 0.7	
	Southeast United States	Not significant	
	Western United States	Not significant	
1996 to 2013	North America, MDN	−1.6 ± 0.3[c,j,n]	This study
1990 to 2012	Western Europe, EMEP	−2.2 ± 0.6	

[a]All trends reported are statistically significant ($P < 0.05$). Data from multiple sources are not synchronous; thus we present snapshots of changes over multiple years and regions where data are available.
[b]Trends were calculated for sites with >5 y of measurements by using monthly median concentrations with the requirement that 75% of the month had valid data.
[c]Based on linear regression.
[d]Annual median concentrations.
[e]Monthly median concentrations.
[f]Daily averaged concentrations.
[g]Seasonal Kendall Test and Sen's slope method.
[h]Stratospheric data and biomass burning plumes filtered based on potential vorticity and CO and ozone concentrations (details provided in methods).
[i]Trend were calculated for monthly mean wet deposition fluxes of sites with at least 75% data coverage.
[j]Annual wet deposition fluxes are used.
[k]Trends are calculated for sites with >5 y of data and >75% valid data coverage.
[l]Weekly wet deposition fluxes were used.
[m]Trends are calculated for sites with >75% data coverage. Monthly precipitation volume-weighted mean concentrations were used.
[n]Sites with at least 10 and 7-y data coverage are selected for MDN and EMEP networks, respectively.

Revised Inventory of Hg Emissions

Standard Hg emission inventories used in atmospheric models (1, 10) indicate flat or increasing trends since 1990, seemingly inconsistent with the observed decreases. Horowitz et al. (2) developed an emission inventory that includes a very large missing source from the atmospheric release of Hg in commercial products. The authors showed that this commercial Hg source peaked in 1970 and has been declining rapidly since, driving an overall global decrease in Hg release to the atmosphere over the 1970-to-2000 period. The authors' inventory still shows an uptick in Hg emissions between 2000 and 2010 attributable to Asian coal-fired utilities and to artisanal and small-scale gold mining (ASGM) in developing countries (1, 19).

Recent work suggests weaker growth in Chinese emissions than previously estimated because of improved data on new coal-fired utilities with flue gas desulfurization (FGD) (20, 21). Also, the increasing trend in ASGM emissions appears to be a spurious effect of improved reporting (9).

Here, we revise Hg emissions and speciation from coal combustion to account for FGD and other emission controls in North America, Europe, Japan, and China. In North America and Europe, coal-fired utilities are the largest remaining atmospheric Hg source (1, 10). Combustion releases both Hg^0, which has a relatively long atmospheric lifetime and is transported globally, and Hg^{II}, which is more likely to deposit regionally. US emissions from coal combustion declined by 75% over 2005 to 2015, mainly
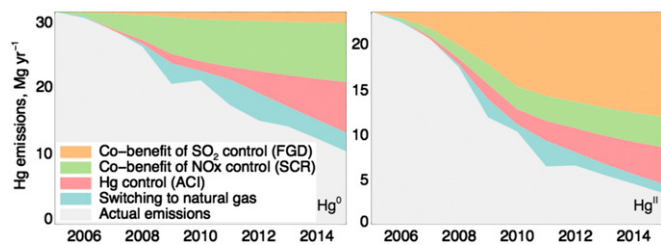
Fig. 1. Major factors driving declines in Hg emission from US coal-fired utilities between 2005 and 2015. Trends were inferred from data on the implementation of different types of emission control technologies.

because of cobenefits from controlling other atmospheric pollutants (Fig. 1). This decrease would be accompanied by a change in the Hg^0/Hg^{II} speciation of emissions that is not recognized in current inventories. Use of FGD to control sulfur dioxide (SO_2) emissions washes out Hg^{II} (22). Use of selective catalytic reduction (SCR) to control nitrogen oxide (NO_x) emissions also oxidizes Hg^0 to Hg^{II}, and application of SCR and FGD in series controls total Hg emissions (23). Activated carbon injection (ACI) to specifically target Hg emissions has also begun to penetrate the energy sector (24). By considering the installation capacity and control efficiency of these devices, we find FGD caused the fraction of total Hg released as Hg^{II} to decline disproportionately to total emissions, from 43% to 24% over the last decade (Fig. 1).

Similar changes in Hg emissions from coal combustion can be inferred for other countries that have implemented air pollution controls and fuel switches over the last two decades. The fraction of coal-fired utilities with FGD increased from 20% to 46% between 1990 to 2002 in Western Europe and from 30% to 70% between 1990 and 2005 in Japan, resulting in a total cumulative decrease of 200 Mg Hg^{II} from developed countries including the US (25, 26). In China, the fraction of coal-fired utilities with FGD capacity increased from zero in 2000 to 86% in 2010, resulting in a drop in annual Hg^{II} emissions of 30% and 250 Mg cumulatively between 1990 and 2010 (21). The growth in energy demand in China has led to a rapid increase in coal combustion (11% y^{-1}), but total Hg emissions over this period increased less (5.8% y^{-1}) because of the implementation of FGD (21). This previously unaccounted shift in speciation implies greater declines in near-field Hg deposition than previously estimated.

Table 2 summarizes our updated global inventory of anthropogenic emissions for 1990 to 2010. The inventory includes revised estimates of emissions from coal combustion as described above, ASGM emissions from Muntean et al. (9), and emissions from commercial products (incineration, volatilization) based on Horowitz et al. (2) (additional details are available in Table S1). Our results indicate a 30% global decline of anthropogenic Hg^0 emissions from 1990 to 2010 (-1.5% y^{-1}). These declines are steepest from 1990 to 2000 but continue through 2010. This contrasts the flat or increasing trends in previous inventories (1, 9, 10). Two-thirds of the decline reflects the phase out of Hg in commercial products. Horowitz et al. (2) previously found that this was offset by rising emissions from coal combustion and ASGM, but our revision to the combustion inventory, as well as the Muntean et al. (9) ASGM inventory, removes the offset.

We find a global increase of 9% in Hg^{II} emissions between 1990 and 2010. This increase is attributable to growth in coal combustion in India and China, with FGD mitigating part of the increase in China. By contrast, Streets et al. estimated a 48% global increase in Hg^{II} emission between 1990 and 2008 (1). The authors did not account for growing implementation of FGD in China because of the lack of necessary information.

Large regional differences in Hg emission trends are apparent from Table 2. The decline in emissions from commercial products has been concentrated in developed countries (2). Total Hg emissions declined by a factor of 6.3 in Western Europe, 3.8 in North America, and 2.0 for other regions of Europe over 1990 to 2010, but emissions in Asia increased by a factor of 1.5.

Consistency with Observed Atmospheric Trends

Fig. 2 shows the 1990-to-2010 trends in atmospheric Hg^0 concentrations and Hg^{II} wet deposition fluxes simulated by the GEOS-Chem (Goddard Earth Observing System-Chemistry) global model using our revised anthropogenic emission inventory and the same meteorological year (to isolate the effect of emissions). Observed trends from Table 1 are also shown. Fig. 3 shows the simulated and observed regional trends averaged across the sites of Table 1.

The model successfully reproduces the observed trends. Declines are largest in North America and Western Europe (-1.5 ± 0.18 to $-2.2 \pm 0.15\%$ y^{-1}), reflecting the particularly large emission decreases in these regions. Shifts in speciation from coal-fired power plants also contribute significantly to the observed decline in wet deposition fluxes. Neglecting this change would result in an underestimate of the trend by a factor of 2 (e.g., ref. 26). The model decline in the free troposphere of the northern hemisphere ($-0.6 \pm 0.037\%$ y^{-1}) reflects a global decrease in total Hg^0 emission (including anthropogenic, natural, and reemission sources) of -0.5% y^{-1}. This decreasing trend is lower than that of anthropogenic Hg^0 emissions (-1.5% y^{-1}) because natural and legacy sources are approximately twice the magnitude of anthropogenic sources and are relatively unchanged. This modeled trend is in the range of observations from CARIBIC ($-0.6 \pm 0.57\%$ y^{-1}) and Mauna Loa Observatory ($-0.9 \pm 0.57\%$ y^{-1}). Model increases are limited to East Asia, consistent with preliminary observations and previous modeling studies (6, 11, 27).

The model decline at northern high latitudes (including one site in North American sector and four in Western Europe) is $-1.3 \pm 0.11\%$ y^{-1}, typical of the northern extratropical background (Fig. 2A), but observations show a much weaker and statistically insignificant decline ($-0.2 \pm 0.5\%$ y^{-1}) (28). A similar discrepancy is observed for wet deposition fluxes over high-latitude regions of Western Europe (Fig. 2C). Fisher and coworkers (29, 30) and Zhang et al. (31) previously showed that trends in the Arctic are complicated by influences from riverine Hg discharges and sea ice cover. A GEOS-Chem simulation by Chen et al. (27), which includes long-term warming temperature and shrinking of Arctic sea ice, indicates that decreased oxidation of Hg^0 and deposition from the atmosphere as well as increased evasion of Hg^0 from the Arctic Ocean offsets the effect of the declining atmospheric background, resulting in no significant trend at high latitudes consistent with observations.

There is substantial uncertainty in current anthropogenic Hg emissions estimates (1, 9, 10, 19). Similar to Streets et al. (1), we calculated lower and upper bounds around the central estimate (Table 2 and Table S1) that correspond to an 80% confidence interval (CI) (the probability of emissions being outside this range is less than 20%). We estimate the resulting uncertainty in emissions is -33% to $+60\%$. However, the calculated emissions trend between 1990 to 2010 is much more consistent, ranging between -1.4% to -0.53% y^{-1} and the propagated uncertainty in the simulated atmospheric trend across years is relatively small ($\pm 20\%$; Fig. 3).

Our results show general agreement between modeled and observed trends on the continental scale (Fig. 3), but the model does not reproduce all fine-scale variability in observations. For example, the model underestimates the atmospheric Hg^0 trend for one site in the western United States and cannot capture the observed increases in Hg^{II} wet deposition near the Four Corners Region in Colorado. These discrepancies are largely caused by

Table 2. Anthropogenic Hg emissions by world region

| Region and emissions	Year of emissions		
	1990, Mg y^{-1}	2000, Mg y^{-1}	2010, Mg y^{-1}
Western Europe			
Hg^0	410	121	61
ASGM	0	0	0
Products	212	77	18
Combustion	198	44	44
Hg^{II}	73	22	15
Total	483 (382–498)	142 (106–228)	77 (57–129)
North America			
Hg^0	399	174	109
ASGM	0	0	0
Products	208	88	66
Combustion	189	85	42
Hg^{II}	70	42	15
Total	469 (361–635)	216 (167–295)	124 (93–175)
Asia and Oceania			
Hg^0	733	812	989
ASGM	81	181	243
Products	288	325	281
Combustion	363	306	465
Hg^{II}	326	358	575
Total	1,060 (774–1,590)	1,170 (806–1,860)	1,560 (1,040–2,530)
Other Europe			
Hg^0	234	126	98
ASGM	7	11	13
Products	42	29	11
Combustion	185	86	75
Hg^{II}	171	101	102
Total	405 (318–658)	227 (173–385)	200 (146–345)
Africa			
Hg^0	166	136	68
ASGM	78	83	28
Products	15	6	0
Combustion	73	46	40
Hg^{II}	67	55	55
Total	233 (151–395)	190 (114–335)	123 (82–216)
Central and South America			
Hg^0	208	174	149
ASGM	110	90	93
Products	64	51	23
Combustion	35	34	33
Hg^{II}	32	39	45
Total	240 (137–406)	214 (126–366)	194 (108–340)
Global			
Hg^0	2,150	1,540	1,480
ASGM	278	366	378
Products	829	576	398
Combustion	1040	600	699
Hg^{II}	739	617	807
Total	2,890 (2,120–4,180)	2,160 (1,490–3,470)	2,280 (1,520–3,730)

Taken from Muntean et al. (9). Products are emissions from use and disposal of commercial products from Horowitz et al. (2). Combustion indicates other and includes coal combustion, cement production, and metal smelting from Streets et al. (1). North America includes the United States and Canada. Mexico is included in Central and South America. Numbers in parenthesis are the 80% CIs.

local emission changes and meteorological effects (26), which are missed by the coarser-resolution simulations used here. More detailed, high-resolution emission inventories and models are required to fully resolve such fine-scale variability in observations.

The influence of changing climate and other environmental factors on the reemissions of Hg from soil and ocean remains unclear (32). The concentrations of major oxidants for atmospheric Hg^0, including OH, O$_3$, and Br, have remained relatively steady or slightly decreased since the mid-1990s and are thus not an important driver for the observed decline (5). Decreasing riverine discharges, which was previously speculated to drive the decline in North Atlantic Ocean Hg concentration and subsequent reemission flux (6), are also insufficient for forcing the global atmospheric trend (31, 33).

Our work has shown that revising anthropogenic emissions with the most up-to-date information can explain the observed
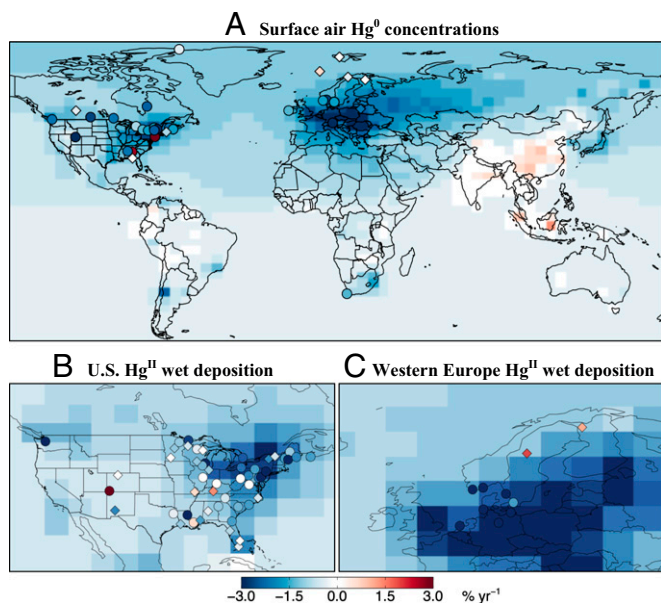
Fig. 2. Trends in atmospheric Hg⁰ concentrations (*A*) and HgII wet deposition fluxes (*B* and *C*) from 1990 to present. Observations from the sites in Table 1 are shown as circles (if trends are statistically significant, $P < 0.05$) and diamonds (not significant). The background shows the trends computed in the GEOS-Chem model driven by our revised 1990 and 2010 anthropogenic emissions inventories from Table 2.

large-scale decline in atmospheric Hg over the past two decades. This finding reinforces the major benefits that have been derived from the phase-out of Hg in many products and emission controls on coal combustion.

Methods

Atmospheric Observations in 1990 to 2010. We include long-term observations (typically >5 y) for atmospheric Hg⁰ concentrations and HgII wet deposition flux at sites worldwide during 1990 to 2014 (Table 1). For all of the measurements,

an ordinary linear regression on the annual means is used to calculate the trend. Because gaseous phase HgII accounts for less than 1–2% of TGM concentrations in surface air, we do not differentiate between Hg⁰ and TGM in ground observations (34). We do not include atmospheric HgII concentrations because long-term records are few and data quality is uncertain (35).

Atmospheric Hg concentration data are available through the Canadian Atmospheric Mercury Network (CAMNet) (eight sites; https://www.ec.gc.ca/natchem), the US Atmospheric Mercury Network (AMNet) (nine sites; nadp.sws.uiuc.edu/amn), and European Monitoring and Evaluation Program (EMEP) (six sites; www.emep.int) networks. We include an analysis of the Hg⁰ data measured at a remote and forested site, Experimental Lake Area, Canada (47.9° N, 93.7° W), during 2005 to 2013. HgII wet deposition fluxes are measured by the Mercury Deposition Network (MDN) (nadp.sws.uiuc.edu/mdn) and the EMEP network over North America and Western Europe, respectively. We select 52 MDN sites with at least 10-y data coverage during 1996 to 2013 and 11 EMEP sites with at least 7-y data since 1990. Atmospheric Hg concentrations have been measured from commercial aircraft by the CARIBIC project since December 2004 (www.caribic-atmospheric.com). We exclude stratospheric data using potential vorticity (European Centre for Medium-Range Weather Forecasts: www.ecmwf.int) and O₃ concentrations (36, 37). We exclude biomass burning plumes if the measured Hg concentration is greater than 2.5 ng m⁻³. Also included here are the Hg⁰ data measured at Mauna Loa Observatory, Hawaii (19.5° N, 155.6° W), during 2002 to 2013, which also samples the free troposphere at an elevation of 3,400 m.

Updated 1990 to 2010 Anthropogenic Emissions. We track the installation of air pollution control devices (FGD, SCR, and ACI) for individual US coal-fired utilities and calculate the associated Hg emission decline and speciation change based on the measured capture efficiencies with different coal types and control device configurations. Fuel type information is obtained from air markets program data by the US Environmental Protection Agency (EPA) (ampd.epa.gov/ampd). The installation time and type of air pollution control devices during 2005 to 2011 are from Mercury and Air Toxics Standards (MATS) Information Collection Request 2011 (www3.epa.gov/ttn/atw/utility/utilitypg.html), with linear extrapolation to 2015 except for ACI, which is from the Institute of Clean Air Companies (www.icac.com). Hg capture efficiencies for different coal types and configuration of control devices are based on US EPA measurements (22). This speciation change over the US is extrapolated to all other developed countries in North America, Western Europe, and Oceania based on their similar trajectory of control technology (24). For China, we follow the change of speciation derived by Zhang et al. (20).

We develop an integrated emission inventory between 1990 and 2010 with decadal resolution, including improved estimates of HgII and Hg⁰ speciation
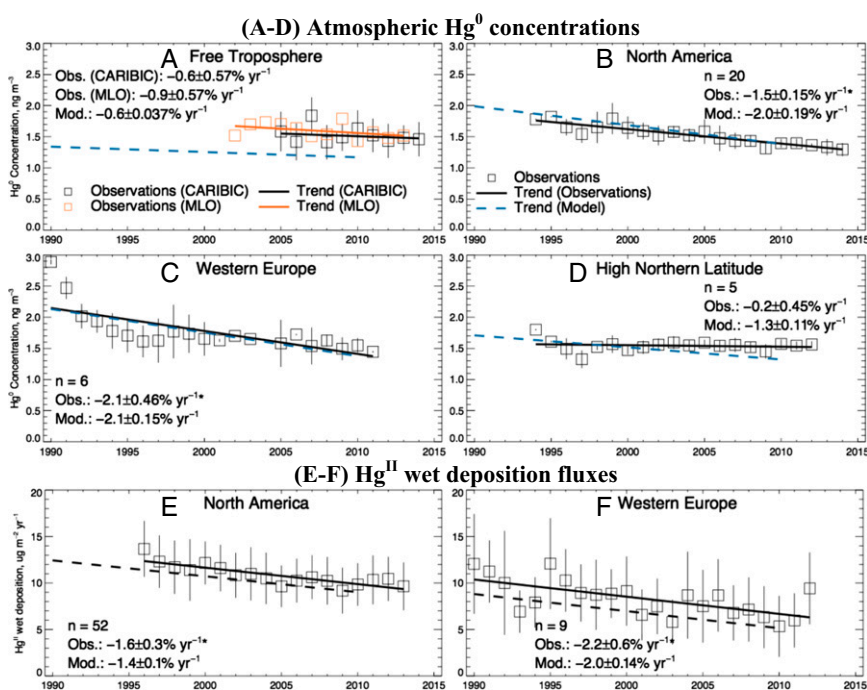
Fig. 3. Regional trends for 1990 to 2013 in atmospheric Hg⁰ concentrations (*A–D*) and HgII wet deposition (*E* and *F*). Observations for individual years are shown as squares with linear regression as solid line. The dashed line is the trend from the GEOS-Chem simulation using our revised anthropogenic emissions inventory for 1990 and 2010 (Table 2). The data are averaged regionally across the sites in Table 1 for the free troposphere (*A*), North America (*B* and *E*), Western Europe (*C* and *F*), and high northern latitude regions (*D*) (vertical bars show the SDs). Regression coefficients (slope ± SE) and number of sites (*n*) are given (*Insets*). The SE of modeled trend is calculated based on the uncertainty range of the emission inventory (Table 2). North American atmospheric Hg⁰ concentrations are from the CAMNet (https://www.ec.gc.ca/natchem) and AMNet (nadp.sws.uiuc.edu/amn) networks and the Experimental Lakes Area, Canada. North American HgII wet deposition is from the MDN (nadp.sws.uiuc.edu/mdn). Observations in Western Europe are from the EMEP network (www.emep.int). High-latitude sites include Alert, Canada and Zeppelin, Norway, and three sites above 60° N from the EMEP network.

from coal-fired utilities as described above. Default emissions are based on those of Streets et al. (1), who provide byproduct emissions from fossil fuel combustion, metal smelting, and waste incineration for 17 world regions. This inventory is updated using more recent country-specific estimates for China in 1995 to 2010 (20, 38), India in 2001 to 2020 (39), the US in 1990 to 2011 [National Emission Inventory (NEI) inventory: www3.epa.gov/ttnchie1/trends], and Western Europe in 1990 (40). We use global atmospheric releases from the use and disposal of commercial products from Horowitz et al. (2) and distribute to different regions based on Hg consumption (10, 18). Regional total emissions from these inventories are distributed on a 1° × 1° grid following the spatial pattern of the Global Emissions InitiAtive (GEIA) inventory (41). For ASGM, we use the Emissions Database for Global Atmospheric Research gridded inventory (9).

Modeled Atmospheric Hg Concentrations and Deposition. The GEOS-Chem Hg model (version 9-01-02) is used to calculate the atmospheric Hg trends driven by Hg emission changes. The model includes a 3D global atmosphere coupled to 2D slab ocean and land models. A detailed description and evaluation of this model is available in Holmes et al. (42), Amos et al. (43), and Zhang et al. (44). The horizontal resolution is 4° latitude × 5° longitude, with 47 vertical layers extending to the mesosphere. Atmospheric transport is driven by assimilated meteorological data from the GEOS-5 of the NASA Global Modeling and Assimilation Office.

The model traces two species: elemental mercury (Hg^0) and divalent mercury (Hg^{II}). Hg^{II} is partitioned thermodynamically between the gas and particle phase on the basis of local temperatures and total aerosol concentration computed with a GEOS-Chem aerosol simulation (43). The model includes the oxidation of Hg^0 by atomic bromine and the photochemical reduction of Hg^{II} in cloud droplets. We do not include the fast reduction of Hg^{II} in coal-fired power plant plumes previously introduced by Zhang et al. (44) and Amos et al. (43) because more recent studies find that the reduction rate is slower than previously estimated (0–55% of emitted Hg^{II} is reduced with a mean value of 4.9%) (45, 46). Redox chemistry also takes place in the surface ocean and soil reservoirs, which receive atmospheric deposition and reemit to atmosphere through land–air and sea–air exchanges.

We conduct 3-y simulations with different anthropogenic emissions corresponding to years 1990 and 2010 (Table 2). The first 2 y are used for initialization, and the third year is used for analysis. The same meteorological year (2008) is used for all simulations to remove the influence of interannual meteorological variability. The soil and subsurface ocean concentrations are kept constant to isolate the impact of changing atmospheric emissions in the recent two decades.

1. Streets DG, et al. (2011) All-time releases of mercury to the atmosphere from human activities. *Environ Sci Technol* 45(24):10485–10491.
2. Horowitz HM, Jacob DJ, Amos HM, Streets DG, Sunderland EM (2014) Historical Mercury releases from commercial products: Global environmental implications. *Environ Sci Technol* 48(17):10242–10250.
3. Mahaffey KR, et al. (2011) Balancing the benefits of n-3 polyunsaturated fatty acids and the risks of methylmercury exposure from fish consumption. *Nutr Rev* 69(9):493–508.
4. Selin NE, et al. (2007) Chemical cycling and deposition of atmospheric mercury: Global constraints from observations. *J Geophys Res* 112(D2):D02308.
5. Slemr F, Brunke EG, Ebinghaus R, Kuss J (2011) Worldwide trend of atmospheric mercury since 1995. *Atmos Chem Phys* 11(10):4779–4787.
6. Soerensen AL, et al. (2012) Multi-decadal decline of mercury in the North Atlantic atmosphere explained by changing subsurface seawater concentrations. *Geophys Res Lett* 39(21):L21810.
7. Cole A, et al. (2014) A survey of mercury in air and precipitation across Canada: Patterns and trends. *Atmosphere* 5(3):635–668.
8. Prestbo EM, Gay DA (2009) Wet deposition of mercury in the US and Canada, 1996-2005: Results and analysis of the NADP mercury deposition network (MDN). *Atmos Environ* 43(27):4223–4233.
9. Muntean M, et al. (2014) Trend analysis from 1970 to 2008 and model evaluation of EDG-ARv4 global gridded anthropogenic mercury emissions. *Sci Total Environ* 494–495:337–350.
10. Wilson S, et al. Arctic Monitoring and Assessment Programme (2010) Updating Historical Global Inventories of Anthropogenic Mercury Emissions to Air. AMAP Technical Report No. 3 (Arctic Monitoring and Assessment Programme, Olso).
11. Slemr F, Brunke EG, Labuschagne C, Ebinghaus R (2008) Total gaseous mercury concentrations at the Cape Point GAW station and their seasonality. *Geophys Res Lett* 35(11):L11807.
12. Slemr F, Scheel HE (1998) Trends in atmospheric mercury concentrations at the summit of the Wank mountain, southern Germany. *Atmos Environ* 32(5):845–853.
13. Weigelt A, et al. (2015) Analysis and interpretation of 18 years of mercury observations since 1996 at Mace Head, Ireland. *Atmos Environ* 100:85–93.
14. Krnavek L, Landis MS, Colton A, Kuniyuki D A study of ambient mercury in the marine free troposphere, Annual Global Monitoring Conference, Boulder, CO, May 18–19, 2010. Available at www.esrl.noaa.gov/gmd/publications/annual_meetings/2010/pdfs/3-Krnavek.pdf.
15. Butler TJ, et al. (2008) Regional precipitation mercury trends in the eastern USA, 1998–2005: Declines in the Northeast and Midwest, no trend in the Southeast. *Atmos Environ* 42(7):1582–1592.
16. Risch MR, et al. (2012) Spatial patterns and temporal trends in mercury concentrations, precipitation depths, and mercury wet deposition in the North American Great Lakes region, 2002-2008. *Environ Pollut* 161:261–271.
17. Fu XW, et al. (2015) Observations of atmospheric mercury in China: A critical review. *Atmos Chem Phys Discuss* 15(8):11925–11983.
18. Amap/Unep (2013) *Technical Background Report for the Global Mercury Assessment 2013* (Arctic Monitoring and Assessment Programme, Oslo/UNEP Chemicals Branch, Geneva).
19. Zhao Y, Zhong H, Zhang J, Nielsen CP (2014) Evaluating the effects of China's pollution control on inter-annual trends and uncertainties of atmospheric mercury emissions. *Atmos Chem Phys* 15(8):4317–4337.
20. Zhang L, et al. (2015) Updated emission inventories for speciated atmospheric mercury from anthropogenic sources in China. *Environ Sci Technol* 49(5):3185–3194.
21. Giang A, Stokes LC, Streets DG, Corbitt ES, Selin NE (2015) Impacts of the minamata convention on mercury emissions and global deposition from coal-fired power generation in Asia. *Environ Sci Technol* 49(5):5326–5335.
22. Bullock D, Johnson S (2011) *Electric Generating Utility Mercury Speciation Profiles for the Clean Air Mercury Rule* (Emissions Inventory and Analysis Group USEPA, Research Triangle Park, NC).
23. Rallo M, Lopez-Anton MA, Contreras ML, Maroto-Valer MM (2012) Mercury policy and regulations for coal-fired power plants. *Environ Sci Pollut Res Int* 19(4):1084–1096.
24. Sloss L, Mercury-related policy developments in the European Union, The 2007 Mercury Control Technology Conference (National Energy Technology Laboratory), Pittsburgh, 11–13 December 2007.
25. Klimont Z, Smith SJ, Cofala J (2013) The last decade of global anthropogenic sulfur dioxide: 2000–2011 emissions. *Environ Res Lett* 8(1):014003.
26. Zhang Y, Jaeglé L (2013) Decreases in mercury wet deposition over the United States during 2004–2010: Roles of domestic and global background emission reductions. *Atmosphere* 4(2):113–131.
27. Chen L, et al. (2015) A decline in Arctic Ocean mercury suggested by differences in decadal trends of atmospheric mercury between the Arctic and northern midlatitudes. *Geophys Res Lett* 42(14):6076–6083.
28. Cole AS, et al. (2013) Ten-year trends of atmospheric mercury in the high Arctic compared to Canadian sub-Arctic and mid-latitude sites. *Atmos Chem Phys* 13(3):1535–1545.
29. Fisher JA, et al. (2013) Factors driving mercury variability in the Arctic atmosphere and ocean over the past thirty years. *Glob Biogeochem Cycles* 27(4):1226–1235.
30. Fisher JA, et al. (2012) Riverine source of Arctic Ocean mercury inferred from atmospheric observations. *Nat Geosci* 5(7):499–504.
31. Zhang Y, et al. (2015) Biogeochemical drivers of the fate of riverine mercury discharged to the global and Arctic oceans. *Global Biogeochem Cycles* 29(6):854–864.
32. Krabbenhoft DP, Sunderland EM (2013) Environmental science. Global change and mercury. *Science* 341(6153):1457–1458.
33. Amos HM, et al. (2014) Global biogeochemical implications of mercury discharges from rivers and sediment burial. *Environ Sci Technol* 48(16):9514–9522.
34. Gustin M, Jaffe D (2010) Reducing the uncertainty in measurement and understanding of mercury in the atmosphere. *Environ Sci Technol* 44(7):2222–2227.
35. Jaffe DA, et al. (2014) Progress on understanding atmospheric mercury hampered by uncertain measurements. *Environ Sci Technol* 48(13):7204–7206.
36. Talbot R, Mao H, Scheuer E, Dibb J, Avery M (2007) Total depletion of Hg in the upper troposphere–lower stratosphere. *Geophys Res Lett* 34(23):L23804.
37. Lyman SN, Jaffe DA (2012) Formation and fate of oxidized mercury in the upper troposphere and lower stratosphere. *Nat Geosci* 5(2):114–117.
38. Wu Y, et al. (2006) Trends in anthropogenic mercury emissions in China from 1995 to 2003. *Environ Sci Technol* 40(17):5312–5318.
39. Burger Chakraborty L, Qureshi A, Vadenbo C, Hellweg S (2013) Anthropogenic mercury flows in India and impacts of emission controls. *Environ Sci Technol* 47(15):8105–8113.
40. Pacyna JM (1997) Mercury and health: Emissions and their reduction strategies in the European region of WHO (Environmental Health Policy and Services, The World Health Organization Regional Office for Europe, Hagan, Norway).
41. Pacyna EG, et al. (2010) Global emission of mercury to the atmosphere from anthropogenic sources in 2005 and projections to 2020. *Atmos Environ* 44(20):2487–2499.
42. Holmes CD, et al. (2010) Global atmospheric model for mercury including oxidation by bromine atoms. *Atmos Chem Phys* 10(24):12037–12057.
43. Amos HM, et al. (2012) Gas-particle partitioning of atmospheric Hg(II) and its effect on global mercury deposition. *Atmos Chem Phys* 12(1):591–603.
44. Zhang Y, et al. (2012) Nested-grid simulation of mercury over North America. *Atmos Chem Phys Discuss* 12:2603–2646.
45. Deeds DA, Banic CM, Lu J, Daggupaty S (2013) Mercury speciation in a coal-fired power plant plume: An aircraft-based study of emissions from the 3640 MW Nanticoke Generating Station, Ontario, Canada. *J Geophys Res Atmos* 118(10):4919–4935.
46. Landis MS, Ryan JV, ter Schure AF, Laudal D (2014) Behavior of mercury emissions from a commercial coal-fired power plant: The relationship between stack speciation and near-field plume measurements. *Environ Sci Technol* 48(22):13540–13548.